

Squeezing-induced Topological Gap Opening on Bosonic Bogoliubov Excitations

Liang-Liang Wan^{1,2}, Zixian Zhou¹, and Zhi-Fang Xu^{1*}

¹*Shenzhen Institute for Quantum Science and Engineering and Department of Physics, Southern University of Science and Technology, Shenzhen 518055, China*

²*School of Physics and Technology, Wuhan University, Wuhan, Hubei 430072, China*

We investigate the role of squeezing interaction in inducing topological Bogoliubov excitations of a bosonic system. We introduce a squeezing transformation which is capable of reducing the corresponding Bogoliubov-de Gennes Hamiltonian to an effective non-interacting one with the spectra and topology unchanged. In the weak interaction limit, we apply the perturbation theory to investigate the squeezing-induced topological gap opening on bosonic Bogoliubov excitations and find that the squeezing interaction plays an equivalent role as a spin-orbit or Zeeman-like coupling in the effective Hamiltonian. We thus apply this formalism to two existed models for providing deeper understandings of their topological structures. We also construct minimal models based on the elegant Clifford algebra for realizing bosonic topological Bogoliubov excitations. Our construction is potentially applicable for experiments in bosonic systems.

I. INTRODUCTION

In this century tremendous progress has been made in the exploration and realization of topological states of matter [1–3]. Besides the famous topological insulators and superconductors [4, 5], topological bosonic systems without fermionic analogy also attract wide attentions [6–10]. It is reported that magnetic materials [11–24], optical systems [25–27], and ultracold atoms [28–32] are capable of supporting topological bosonic Bogoliubov excitations (BEs) with nontrivial Chern numbers or \mathbb{Z}_2 invariants. These systems are described by a bosonic Bogoliubov-de Gennes (BdG) model which is adaptive to the peculiar symplectic/pseudo-unitary diagonalization [33–35]. Recent works further show that their topological classification is different from the common Atland-Zirnbauer (AZ) class [21, 36–41]. Moreover, the edge state of the bosonic BEs as a typical topological effect is also predicted [11–15, 19, 24–31, 42].

The bosonic BdG Hamiltonian is a mean-field description of a bosonic system with a weak nonlinear interaction [33, 34]. It consists of a single-particle dispersion term and a bi-particle annihilation/creation interaction known as the two-mode squeezing [43]. As a vast difference from the fermionic case, the Bogoliubov transformation preserving the bosonic commutation relation belongs to a non-compact pseudo-unitary group [44]. This brings difficulty in the analysis of the BE modes and spectra. For this reason, previous studies usually resort to numerical computations and are unable to give a clear understanding on the topological origin of BEs with squeezing interaction. Besides, these sporadic examples [11–32] do not provide a systematical way to construct such topological BEs. The essential problem here is the missing of an intuitive picture that depicts the role of squeezing in the BE spectra.

In this article, we look for a concise formula that char-

acterizes the topological BEs of bosonic BdG systems in the weak interaction limit. Our exploration starts with a fact that the bosonic BdG Hamiltonian can be continuously deformed onto a non-interacting one with the same BE spectra and topology. We reveal that the non-interacting Hamiltonian is nothing but the squeezed state representation of the original model and acts as an effective Hamiltonian. In its explicit expression, the perturbative squeezing interaction can be linearized as an effective spin-orbit coupling (SOC) added to the dispersion term. This result translates the topological analysis and construction of bosonic BdG model to those of single-particle one belonging to the AZ class [37, 38].

Based on this discovery, we notice that the present topological bosonic BEs are of a unified construction. In those models the dispersion part usually corresponds to a gapless band structure while the presence of squeezing interaction opens a bulk gap in the high-lying BE spectra. The construction has been applied to many topological band models and can be viewed as a variation of the band-inversion [45–48] phenomenon. In this situation, we find that the squeezing-induced SOC in the effective Hamiltonian can be further approximated as a momentum-independent Zeeman-like coupling. If the model is made up of Dirac matrices, it can even be reduced to a constant mass term. Therefore, the topological effect of squeezing has a clear fermionic analogy and interpretation. This provides us a deeper understanding toward the squeezing-induced topological gap on bosonic BEs.

As another motivation of this work, we also search for the minimal construction of topological bosonic BEs. Like the Atiyah-Bott-Shapiro construction for free-fermion systems [38, 49], here we utilize the Clifford algebra to yield the bosonic BdG Hamiltonian including both the dispersion and squeezing terms. A squeezing-induced gap is also designed to generate topological BE bands. Despite of the difficulty in solving the exact BE spectra, our effective Hamiltonian takes an elegant Dirac form and faithfully reflects the origin of topology. This minimal construction is capable of systematically producing topo-

* xuzf@sustech.edu.cn

logical bosonic BEs by converting the fermionic topological insulator into the bosonic version. The method will also inspire more realistic models for experiments in the future.

The rest of article is organized as follows. In Sec. II, the bosonic BdG model and its effective Hamiltonian are introduced. In Sec. III, perturbation formula of squeezing-induced topological gap is derived and applied to discussing two existed models. In Sec. IV, the minimal construction of topological bosonic BE is built and two nontrivial models are designed. In Sec. V conclusions are made.

II. MODEL AND EFFECTIVE HAMILTONIAN

We consider the bosonic BdG model which describes a bosonic system with a nonlinear interaction after the mean-field approximation [33, 34, 50]. This model is available in various physical systems including magnonic crystal [12, 13, 15, 22, 23], photonic crystal [26, 51, 52], and ultracold atoms in optical lattice [28–32, 53–55]. The BdG Hamiltonian contains a dispersion term $\sum_{\mathbf{k}} \hat{\mathbf{a}}_{\mathbf{k}}^\dagger H_a(\mathbf{k}) \hat{\mathbf{a}}_{\mathbf{k}}$ that originates from the single-particle system and a part of interaction [30–32]. It also contains a squeezing interaction $\frac{1}{2} \sum_{\mathbf{k}} \hat{\mathbf{a}}_{\mathbf{k}}^\dagger H_s(\mathbf{k}) \hat{\mathbf{a}}_{-\mathbf{k}}^{\dagger\top} + \text{h.c.}$ that is reduced from the rest part of interaction. Here $\hat{\mathbf{a}}_{\mathbf{k}}^\dagger = (\hat{a}_{\mathbf{k},1}^\dagger, \dots, \hat{a}_{\mathbf{k},N}^\dagger)$ is a multi-component bosonic creation operator with regard to d -dimensional momentum \mathbf{k} , and $\hat{\mathbf{a}}_{\mathbf{k}}^{\dagger\top}$ transposes these elements (operators $\hat{a}_{\mathbf{k},i}^\dagger$) to a column vector. The complete BdG Hamiltonian can be concisely written as

$$\hat{H} = \frac{1}{2} \sum_{\mathbf{k}} \hat{\phi}_{\mathbf{k}}^\dagger H(\mathbf{k}) \hat{\phi}_{\mathbf{k}}, \quad (1)$$

with field operator $\hat{\phi}_{\mathbf{k}}^\dagger = (\hat{\mathbf{a}}_{\mathbf{k}}^\dagger, \hat{\mathbf{a}}_{-\mathbf{k}}^\top)$ and $2N \times 2N$ Hermitian matrix

$$H(\mathbf{k}) = \begin{pmatrix} H_a(\mathbf{k}) & H_s(\mathbf{k}) \\ H_s^*(-\mathbf{k}) & H_a^*(-\mathbf{k}) \end{pmatrix}. \quad (2)$$

In this system, there is an intrinsic particle-hole symmetry [13, 26, 40, 41, 56] which reads

$$U_C^{-1} H^*(-\mathbf{k}) U_C = H(\mathbf{k}), U_C = \begin{pmatrix} & I_N \\ I_N & \end{pmatrix}, \quad (3)$$

where I_N denotes the $N \times N$ identity matrix. Besides, we require the energy non-negative (i.e., $H(\mathbf{k})$ positive semi-definite) to guarantee the thermodynamic stability.

Before discussing the topology of BEs, we first need to solve the BEs by a Bogoliubov transformation V that preserves the bosonic commutation relation

$$\left[\hat{\phi}_{\mathbf{k},i}, \hat{\phi}_{\mathbf{k},j}^\dagger \right] = \tau_{ij}, \tau = \begin{pmatrix} I_N & \\ & -I_N \end{pmatrix}, \quad (4)$$

i.e., $V^\dagger \tau V = \tau$. It has been known that V forms a non-compact pseudo-unitary group $U(N, N)$. This has a vast

difference from the unitary group used to diagonalize a fermionic system. Nevertheless, the traditional approach leads to implicit solutions and cannot reveal the effect of squeezing plainly. Instead, we adopt a squeezing transformation which is capable of explicitly transforming the BdG Hamiltonian to a non-interacting one [43]. The effective non-interacting Hamiltonian will not only give the BE modes and spectra via a common unitary diagonalization but also present the effect of squeezing in an intuitive way.

To be more specific, we define a squeeze operator

$$\hat{S} = \exp \sum_{\mathbf{k}} \frac{1}{2} \left[\mathbf{a}_{\mathbf{k}}^\dagger w(\mathbf{k}) \mathbf{a}_{-\mathbf{k}}^{\dagger\top} - \text{h.c.} \right], \quad (5)$$

with a natural constraint $w^\top(\mathbf{k}) = w(-\mathbf{k})$. By using commutation relation

$$\left[\hat{\phi}_{\mathbf{k},i}, \ln \hat{S} \right] = \left[W(\mathbf{k}) \hat{\phi}_{\mathbf{k}} \right]_i, W = \begin{pmatrix} & w \\ w^\dagger & \end{pmatrix}, \quad (6)$$

we introduce a unitary transformation

$$\hat{S}^\dagger \hat{\phi}_{\mathbf{k}} \hat{S} = e^{W(\mathbf{k})} \hat{\phi}_{\mathbf{k}}. \quad (7)$$

The field operator after transformation is a linear superposition of $\hat{\mathbf{a}}_{\mathbf{k}}$ and $\hat{\mathbf{a}}_{-\mathbf{k}}^\dagger$, which still keeps the commutation relation (4). This implies that the squeezing transformation is a special Bogoliubov transformation. Then the Hamiltonian in the squeezed-state representation is given by

$$\hat{S}^\dagger \hat{H} \hat{S} = \frac{1}{2} \sum_{\mathbf{k}} \hat{\phi}_{\mathbf{k}}^\dagger h(\mathbf{k}) \hat{\phi}_{\mathbf{k}}, \quad (8)$$

where

$$h(\mathbf{k}) = e^{W(\mathbf{k})} H(\mathbf{k}) e^{W(\mathbf{k})}. \quad (9)$$

To some extent, $h(\mathbf{k})$ and $H(\mathbf{k})$ are physically equivalent since they are connected via a congruent transformation.

By choosing a special $W(\mathbf{k})$ we can make $h(\mathbf{k})$ block-diagonal, that is $\tau h \tau = h$. Using the identity $\tau W \tau = -W$, we can infer that the block-diagonal condition is equivalent to $\tau H \tau = \exp(2W) H \exp(2W)$ whose solution is given by [41]

$$e^{2W} = H^{-\frac{1}{2}} \left(H^{\frac{1}{2}} \tau H \tau H^{\frac{1}{2}} \right)^{\frac{1}{2}} H^{-\frac{1}{2}}. \quad (10)$$

Since H is positive definite (thermodynamic stability), $H^{\pm 1/2}$ are well defined. Also, $H^{1/2} \tau H \tau H^{1/2} = (H^{1/2} \tau H^{1/2})^2$ is positive definite, then its square root is well defined, too. If H encounters a zero energy, one may utilize $H + 0^+ \cdot I$ instead of H and solve the limit of h .

Combining Eqs. (3), (9) and (10), we find that the particle-hole symmetry is inherited by $h(\mathbf{k})$, i.e.,

$$h(\mathbf{k}) = U_C^{-1} h^*(-\mathbf{k}) U_C = \begin{pmatrix} h_a(\mathbf{k}) & \\ & h_a^*(-\mathbf{k}) \end{pmatrix}. \quad (11)$$

We emphasize that the above treatment is equivalent to that of Ref. [41]. But the language of second quantization applied here gives a clear physical interpretation, the BdG Hamiltonian in the squeezed state representation is reduced to an effective non-interacting one

$$\hat{S}^\dagger \hat{H} \hat{S} = \sum_{\mathbf{k}} \hat{\mathbf{a}}_{\mathbf{k}}^\dagger h_a(\mathbf{k}) \hat{\mathbf{a}}_{\mathbf{k}}. \quad (12)$$

Now we can easily achieve the BE modes and spectra of \hat{H} by the unitary diagonalization of $h_a(\mathbf{k})$. The BE modes are the eigenstates of the effective non-interacting system after a squeezed-state transformation, and the excitation spectra are simply the eigenvalues of $h_a(\mathbf{k})$.

The squeezing transformation can also be applied to a more generic quadratic bosonic Hamiltonian without the particle-hole symmetry [41]. The obtained effective non-interacting Hamiltonian would contain two isolated parts. Details are given in Appendix A.

The topological relation between the original and effective Hamiltonians has been already revealed in Ref. [41]. Since the squeezing transformation \hat{S} can always be deformed into an identity operator in a trivial way, $H(\mathbf{k})$ can be continuously deformed onto $h(\mathbf{k})$ while keeping the excitation gap opened and the symmetry invariant. This means that they are homotopy equivalent. As a result, the topological structure of H is identical to that of gapped non-interacting system $h_a(\mathbf{k})$, characterized by the AZ class [3, 37, 38]. Therefore, we only focus on $h_a(\mathbf{k})$ instead of \hat{H} in the following discussions. Then the topological analysis of bosonic BEs is converted to that of fermionic topological insulator.

III. PERTURBATION FORMULATION

In this section, we aim to clarify the key role of the squeezing interaction in inducing the topological gap opening on high-lying BEs by using perturbation theory. As shown in Sec. II, the effect of squeezing has been encoded in the expression of effective Hamiltonian $h_a(\mathbf{k})$. Despite of the complicated form, linearization of $H_s(\mathbf{k})$ can be made in the squeezing transformation when the squeezing interaction is weak. As a result, a more concise formula of $h_a(\mathbf{k})$ will be achieved after perturbation truncation and a clearer physical picture will be disclosed.

Firstly, Eq. (9) can be expanded with regard to W and expressed as

$$h = H + \{W, H\} + \frac{1}{2} \{W, \{W, H\}\} + \dots \quad (13)$$

Up to main order, the off-diagonal block of the equation reads

$$0 = H_a w + w H_b + H_s, \quad (14)$$

where we have defined $H_b(\mathbf{k}) \equiv H_a^*(-\mathbf{k})$ and omitted \mathbf{k}

in the expression. And the diagonal block of the expansion formula can be simplified as

$$h_a = H_a + \frac{1}{2} (H_s w^\dagger + w H_s^\dagger), \quad (15)$$

with the help of Eq. (14). It implies that the perturbative squeezing interaction acts as an effective SOC $H_{\text{SOC}}(\mathbf{k}) \equiv (H_s w^\dagger + w H_s^\dagger)/2$, which is added to the zeroth-order dispersion term $H_a(\mathbf{k})$ in the effective Hamiltonian $h_a = H_a + H_{\text{SOC}}$, since $H_{\text{SOC}}(\mathbf{k})$ involves the (quasi-)momentum \mathbf{k} as well as internal degrees of freedom including sublattices, atomic orbitals and even spins. After some algebra, the explicit expression of effective Hamiltonian in the $H_{a,b}$ -representation is then shown up,

$$\begin{aligned} (g_a^\dagger h_a g_a)_{ij} &= D_{ai} \delta_{ij} - \frac{1}{2} \left[g_a^\dagger H_s (D_{ai} I + H_b)^{-1} H_s^\dagger g_a \right]_{ij} \\ &\quad - \frac{1}{2} \left[g_a^\dagger H_s (D_{aj} I + H_b)^{-1} H_s^\dagger g_a \right]_{ij}, \end{aligned} \quad (16)$$

where $D_{a,b} = g_{a,b}^\dagger H_{a,b} g_{a,b}$ are the diagonal matrices of eigenenergies of $H_{a,b}$, $g_{a,b}$ are the unitary matrices and the subscripts i, j denote the band indices. In Eq. (16), we have substituted the unique solution, $(g_a^\dagger w g_b)_{ij} = -(H_s)_{ij} / (D_{ai} + D_{bj})$. Since w is unique, the paraunitarity of e^W is automatically guaranteed. The squeezing-induced SOC described by the last two terms records the virtual processes of bi-particle creation/annihilation and annihilation/creation which are provoked by the squeezing interaction $\frac{1}{2} \hat{\mathbf{a}}_{\mathbf{k}}^\dagger H_s(\mathbf{k}) \hat{\mathbf{a}}_{-\mathbf{k}}^\dagger + \text{h.c.}$

The formula of Eq. (16), however, is too complex to grasp its profoundness. It is expected to simplify via a slight deformation with the topological feature unchanged. We first consider a boring case that the dispersion term $H_a(\mathbf{k})$ already has a finite band gap on high-lying excitation. In this case, infinitesimal squeezing term $H_s(\mathbf{k})$ can be arbitrarily modified or even neglected. In the following, we focus on another novel case that a band-crossing point of $H_a(\mathbf{k})$ (labeled by (\mathbf{p}, λ) in the momentum-energy space) is split by the squeezing interaction $H_s(\mathbf{k})$, with a bulk gap opened in the BE bands. This is similar to the band-inversion phenomenon in fermionic topological insulators [45–47, 57, 58] and has covered most existed examples of topological bosonic BEs [26, 30–32]. For simplicity, we merely discuss the case that the gap is opened from a single excitation band-crossing point.

Our strategy of simplification is to precisely characterize the BE bands around the gap-opening point (\mathbf{p}, λ) but slightly deform the band structure elsewhere. This treatment grasps the key topological origin that is the squeezing-induced gap opening. According to the perturbation theory, the first-order correction toward the zeroth-order degenerate point (\mathbf{p}, λ) is determined by block matrix

$$(g_a^\dagger h_a g_a)_{ij} = D_{ai} \delta_{ij} - \left[g_a^\dagger H_s (\lambda I + H_b)^{-1} H_s^\dagger g_a \right]_{ij}, \quad (17)$$

where i and j are confined on the degenerate levels, i.e., $D_{ai}(\mathbf{p}) = D_{aj}(\mathbf{p}) = \lambda$. Up to the main order, the energy splitting of (\mathbf{p}, λ) is accurately characterized by this formula. As for the points away from (\mathbf{p}, λ) , the correction from squeezing is tiny and can be neglected or deformed in a topological sense. Therefore, it is feasible to extend Eq. (17) to the whole bands (i, j running throughout the band indices), arriving at an approximate formula

$$h_a(\mathbf{k}) = H_a(\mathbf{k}) - \left[H_s (\lambda I + H_b)^{-1} H_s^\dagger \right]_{\mathbf{k}=\mathbf{p}}. \quad (18)$$

Note that the squeezing-induced correction $H_s (\lambda I + H_b)^{-1} H_s^\dagger$ becomes \mathbf{k} -independent. It thus can be interpreted as an effective Zeeman coupling. Equation (18) is the key formula to understand the squeezing-induced topological gap on bosonic BEs. Its applications and validity will be shown in two examples below.

A. Example of photonic crystal

Firstly, we revisit topological BEs in photonic crystal with a kagome lattice structure [26], as shown in Fig. 1(a). It starts with a dielectric material containing periodic pores that cause photonic band structure [59]. In the presence of crystalline defects in an appropriate pattern, localized modes would appear and a tight-binding model could be utilized to describe the system. Meanwhile, the nonlinear effect from $\chi^{(2)}$ optical medium would induce an onsite squeezing interaction with the help of an auxiliary driving light [43]. Via the rotating-wave approximation of the driving field, the total Hamiltonian is given by a bosonic BdG Hamiltonian. The dispersion and squeezing terms are given by

$$H_a(\mathbf{k}) = J \begin{pmatrix} \omega/J & 1 + e^{-i\mathbf{k}\cdot\mathbf{l}_3} & 1 + e^{i\mathbf{k}\cdot\mathbf{l}_2} \\ & \omega/J & 1 + e^{-i\mathbf{k}\cdot\mathbf{l}_1} \\ \text{h.c.} & & \omega/J \end{pmatrix}, \quad (19)$$

$$H_s \equiv s \begin{pmatrix} 1 & & \\ & e^{i2\pi/3} & \\ & & e^{-i2\pi/3} \end{pmatrix}, \quad (20)$$

where ω is the on-site energy, J denotes the nearest-neighbor hopping amplitude, and s is the squeezing intensity. Here $\mathbf{k} = (k_x, k_y)$ is the crystal momentum, and $\mathbf{l}_1 = (1, 0)$, $\mathbf{l}_2 = (-1/2, \sqrt{3}/2)$, $\mathbf{l}_3 = (-1/2, -\sqrt{3}/2)$ are lattice vectors (for simplicity, the crystal constant is assumed to be 1.). The on-site squeezing interaction shows a phase distribution in the internal space which is the key for generating the topological BE.

The energy spectra of $H_a(\mathbf{k})$ is gapless as shown in Fig. 1(c). There are two Dirac points at (K, λ_K) , $(K', \lambda_{K'})$ and a quadratic band-crossing point at (Γ, λ_Γ) . The BE spectra given by the eigenvalues of $h_a(\mathbf{k})$ are numerically calculated via Eqs. (9–10), which are shown by the black solid lines in Fig. 1(d). We infer that the squeezing interaction splits all the degenerate points and generates

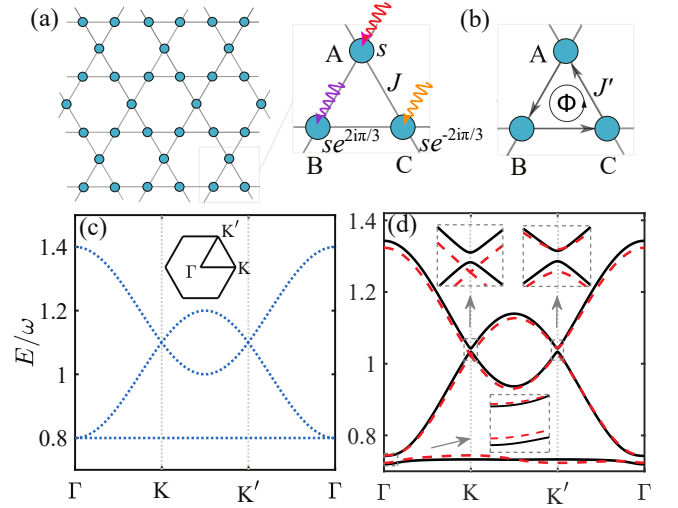


Figure 1. (color online) (a) Sketch of photonic kagome lattice with squeezing interaction. The panel shows the squeezing interaction pattern and hopping coupling. (b) A triangular plaquette of effective model (22) with hopping J' , which has a nontrivial flux Φ . Band structures of (c) $H_a(\mathbf{k})$ and (d) $h_a(\mathbf{k})$ for the photonic crystal. In (c), the hexagon denotes the first Brillouin zone. In (d), the black solid and red dashed lines denote the exact and approximate BE spectra, respectively. Here, $J = 0.1\omega$ and $s = 0.35\omega$.

two bulk excitation gaps opening at Γ , K , K' points. We focus on the lowest excitation band and characterize the squeezing-induced gap around (Γ, λ_Γ) by Eq. (18). After substituting $(\mathbf{p}, \lambda) = (\Gamma, \lambda_\Gamma) = (\mathbf{0}, \omega - 2J)$ into the formula, we find that the effective non-interacting Hamiltonian is described by

$$h_a(\mathbf{k}) = H_a(\mathbf{k}) + J \begin{pmatrix} -\epsilon/J & z & z^* \\ z^* & -\epsilon/J & z \\ z & z^* & -\epsilon/J \end{pmatrix}, \quad (21)$$

with $\epsilon = |s|^2 \omega/2 (\omega^2 - J\omega - 2J^2)$ and $z = (\epsilon/\omega) \exp(-i2\pi/3)$. Its spectra are denoted by the red dashed line in Fig. 1(d). We find that the approximate result fits the exact solution well, especially near the original band-crossing point (Γ, λ_Γ) . The Chern number for lowest BE band is -1 . In addition, it is worthy to mention that the analytical result disagrees at K point since the perturbation applied around Γ point works for the low-lying BEs and is not responsible for the high-lying BEs.

The value of Chern number can be analytically understood as follows. At the symmetry point Γ , the effective Hamiltonian $h_a(\mathbf{k} = \Gamma)$ shows that each nearest-neighbor hopping given by $J(1 + z/2)$ possesses a phase $\arg(1 + z/2)$ and an flux $\Phi = 3 \arg(1 + z/2)$ is accumulated for each triangular plaquette. This can be extended from the symmetry point Γ to the whole Brillouin zone in the sense of topology. Therefore, we achieve a new model, as shown in Fig. 1(b), by making a slight deformation $z \mapsto z(1 + e^{-i\mathbf{k}\cdot\mathbf{l}_i})/2$ for the squeezing-induced

SOC term in Eq. (21). And it is governed by the Hamiltonian

$$h'_a(\mathbf{k}) = \begin{pmatrix} \omega - \epsilon & J'(1 + e^{-i\mathbf{k}\cdot\mathbf{l}_3}) & J'^*(1 + e^{i\mathbf{k}\cdot\mathbf{l}_2}) \\ & \omega - \epsilon & J'(1 + e^{-i\mathbf{k}\cdot\mathbf{l}_1}) \\ \text{h.c.} & & \omega - \epsilon \end{pmatrix}, \quad (22)$$

where the nearest-neighbor hopping amplitude is given by $J' = J(1 + z/2)$. This would not affect the squeezing-induced topological gap at $\mathbf{k} = \mathbf{0}$ (Γ point) such that $h_a(\mathbf{k})$ and $h'_a(\mathbf{k})$ have the same topological number. We notice that $h'_a(\mathbf{k})$ corresponds to an Ohgushi-Murakami-Nagaosa model [60] which has been well studied. It has a nonvanishing flux per triangular plaquette given by $\Phi = 3 \arg(1 + e^{-i2\pi/3}\epsilon/2\omega)$ which breaks the time-reversal (T) symmetry, while the net flux is zero. Its Chern number is then given by $C = \text{sgn}(\sin \Phi) = -1$ [60] in the weak squeezing regime. Our analysis also confirms the result that the squeezing interaction can be reduced to an effective hopping [25].

B. Example of ultracold atoms in optical lattice

Next, we revisit another model where bosonic atoms are loaded into the second band of a square optical lattice [32], as shown in Fig. 2(a). Focusing on the p -orbitals, the single-particle Hamiltonian is then given by

$$\begin{aligned} H_0(\mathbf{k}) &= (J_3 + J_4)(\cos k_x + \cos k_y) I_4 + \delta\sigma_z \otimes I_2 \\ &+ (J_3 - J_4)(\cos k_x - \cos k_y) I_2 \otimes \sigma_z \\ &+ 4J_1 \cos \frac{k_x}{2} \cos \frac{k_y}{2} \sigma_x \otimes I_2 \\ &- 4J_2 \sin \frac{k_x}{2} \sin \frac{k_y}{2} \sigma_x \otimes \sigma_x. \end{aligned} \quad (23)$$

Here $\sigma_{x,z}$ are the conventional Pauli matrices. 2δ is the offset energy of the double-well. J_1 and J_2 are the amplitudes of the nearest-neighbor hopping, while J_3 and J_4 are the ones of next-nearest-neighbor hopping. (We set the length of lattice vector as 1 for simplicity.) The interaction among atoms generates a spontaneous time-reversal symmetry breaking, leading to a chiral bosonic superfluid [61]. Then after a mean-field approximation, the BEs on top of the chiral superfluid are described by a bosonic BdG Hamiltonian. As a difference from the above photonic crystal model, the complete gapless dispersion term $H_a(\mathbf{k})$ here contains the tight-binding Hamiltonian $H_0(\mathbf{k})$ and also the contribution from the contact atomic interaction. The dispersion and squeezing

terms of the BdG Hamiltonian are given by

$$\begin{aligned} H_a(\mathbf{k}) &= H_0(\mathbf{k}) + \omega I_4 + \Delta\sigma_z \otimes I_2 \\ &= [\omega + (J_3 + J_4)(\cos k_x + \cos k_y)] I_4 \\ &+ (\Delta + \delta)\sigma_z \otimes I_2 \\ &+ (J_3 - J_4)(\cos k_x - \cos k_y) I_2 \otimes \sigma_z \\ &+ 4J_1 \cos \frac{k_x}{2} \cos \frac{k_y}{2} \sigma_x \otimes I_2 \\ &- 4J_2 \sin \frac{k_x}{2} \sin \frac{k_y}{2} \sigma_x \otimes \sigma_x, \end{aligned} \quad (24)$$

$$H_s \equiv -s_1\sigma_z \otimes \sigma_z + is_1 I_2 \otimes \sigma_x - s_2 I_2 \otimes \sigma_z + is_2 \sigma_z \otimes \sigma_x, \quad (25)$$

where $s_{1,2}$ are the interaction intensities and $\Delta = 4s_2$, and ω is the parameter depending on both the tight-binding model and atomic interaction.

The energy spectra of $H_a(\mathbf{k})$ and $h_a(\mathbf{k})$ are presented in Fig. 2(a-b), respectively. We see that $H_a(\mathbf{k})$ is gapless, while $h_a(\mathbf{k})$ has a high-lying excitation gap opened by the squeezing interaction. We then calculate the approximate BE spectra based on Eq. (18) and present the result by the red dashed lines shown in Fig. 2(b). It coincides with the exact solution (black solid lines) in most area, except the vicinity of zero energy at K point ($\mathbf{k} = (\pi, \pi)$). Whereas, the Goldstone mode far away from the gap is unimportant for our topological analysis. The Chern number of the excitation bands below the gap is -2 .

Interestingly, in the single-particle picture, the band structure of $H_0(\mathbf{k})$ is gapped [32], while the contribution of interaction to $H_a(\mathbf{k})$ results in the dispersion gapless, and the presence of the squeezing interaction H_s opens a high-lying topological excitation gap. In other words, the interaction-driven topological model must experience the process of gap closing-and-opening. This topological phase transition can be understood in the framework of AZ class [3, 37, 38] since the effective model $h_a(\mathbf{k})$ is non-interacting. In $h_a(\mathbf{k})$, the term $\Delta\sigma_z \otimes I_2$ contributed from interaction closes the band gap shown in Fig. 2(b). And then the squeezing-induced Zeeman coupling breaks the time-reversal symmetry and opens an excitation gap at (\mathbf{p}, λ) point shown in Fig. 2(c). It acts as the role of band-inversion [45–48] and results in the nonvanishing Chern number.

Till now, the validity and power of Eq. (18) have been verified. It lays a foundation for analyzing and constructing topological bosonic BEs.

IV. MINIMAL CONSTRUCTIONS

In this section, we search for the minimal construction of both \mathbb{Z} -type and \mathbb{Z}_2 -type topological bosonic BEs. The minimal model is expected to be analytically solvable with an intuitive physical picture. This is beneficial to exploring more complicated model in realistic experiments. Like the simplest free-fermion models [38], we

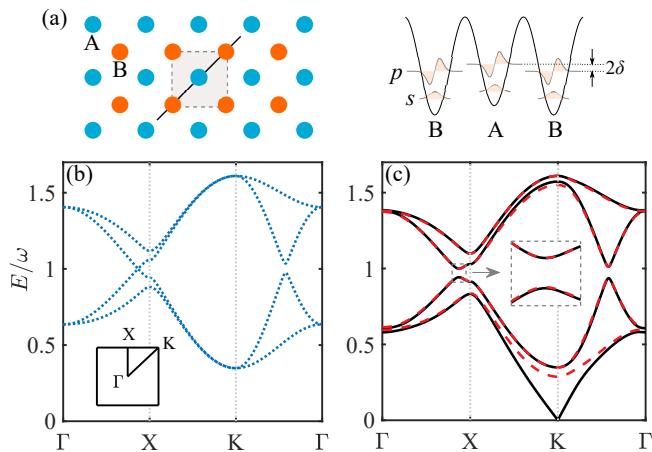


Figure 2. (color online) (a) Sketch of the optical square lattice loaded cold atoms [32]. The dashed square denotes the unit cell. The right panel shows the optical potential along the direction of the black solid line. Band structure of (b) $H_a(\mathbf{k})$ and (c) $h_a(\mathbf{k})$. In (b), the square denotes the Brillouin zone. In (c), the black solid and red dashed lines denote the exact and approximate BE spectra, respectively. The parameters are given by $J_1 = 0.0555E_R$, $J_2 = 0.0912E_R$, $J_3 = 0.0158E_R$, $J_4 = -0.0098E_R$, $\delta = 0.06E_R$, $\omega = 0.5789E_R$, $s_1 = 0.1E_R$, $s_2 = -0.0106E_R$ and E_R is the recoil energy of ^{87}Rb atom, which are the same as Ref. [32].

adopt the elegant Clifford algebra to build a two-band bosonic BdG Hamiltonian. Meanwhile, a momentum-independent squeezing interaction is designed for generating topological BEs. To be more specific, $H_a(\mathbf{k})$ is assumed to be

$$H_a(\mathbf{k}) = \lambda I + \mathbf{r}(\mathbf{k}) \cdot \boldsymbol{\gamma}, \quad (26)$$

where $\mathbf{r}(\mathbf{k}) = (r_1, r_2, \dots)$ is a set of real functions of \mathbf{k} and $\boldsymbol{\gamma} = (\gamma_1, \gamma_2, \dots)$ is a set of Clifford generators satisfying $\{\gamma_m, \gamma_n\} = 2\delta_{mn}I$. The domain of \mathbf{k} can either be a compactified Euclidean space $\mathbb{R}^d \cup \infty = S^d$ (for free-propagating bosons) or reciprocal space T^d (for lattice models). We further assume one band-crossing point determined by $\mathbf{r}(\mathbf{p}) = \mathbf{0}$ which locates at a inversion-invariant (crystal) momentum $\mathbf{p} = -\mathbf{p}$. The squeezing interaction is chosen as the simplest on-site interaction

$$H_s \equiv \xi I + \mathbf{s} \cdot \boldsymbol{\gamma}, \quad (27)$$

where ξ is a complex number and \mathbf{s} is a real vector satisfying $(\mathbf{s} \cdot \boldsymbol{\gamma})^\top = \mathbf{s} \cdot \boldsymbol{\gamma}$. The transpose symmetry $H_s = H_s^\top$ guarantees that $H(\mathbf{k})$ obeys the particle-hole symmetry described by Eq. (3).

Applying the perturbation theory discussed in Sec. III, we obtain the effective non-interacting Hamiltonian which is given by

$$h_a(\mathbf{k}) = \eta I + \mathbf{r}(\mathbf{k}) \cdot \boldsymbol{\gamma} - \frac{\text{Re}\xi}{\lambda} \mathbf{s} \cdot \boldsymbol{\gamma}, \quad (28)$$

where $\eta = \lambda - (|\xi|^2 + \|\mathbf{s}\|^2)/2\lambda$. The squeezing-induced correction simply reduces to a mass term $-\text{Re}\xi(\mathbf{s} \cdot \boldsymbol{\gamma})/\lambda$,

which opens a topological excitation gap around the original band-crossing point, e.g. Dirac point. We immediately infer that the effective Hamiltonian of bosons reproduces the minimal construction of fermionic topological insulators. We can utilize the well-studied fermionic models to create the related bosonic versions for generating topological BEs, and two examples are given below.

A. \mathbb{Z} -type topological BE

Firstly, we attempt to construct a two-dimensional bosonic BdG model which supports a \mathbb{Z} -type topological BE. The Hamiltonian has no other symmetry except the intrinsic particle-hole symmetry and the topological invariant of $h_a(\mathbf{k})$ is characterized by a Chern number. The Hamiltonian in form of Eqs. (26–27) is set as [62]

$$\mathbf{r}(\mathbf{k}) = J(\sin k_x, \sin k_y, \cos k_x + \cos k_y), \quad (29)$$

and $\mathbf{s} = (0, 0, s)$. The Clifford generators are chosen as Pauli matrices, i.e., $\boldsymbol{\gamma} = (\sigma_1, \sigma_2, \sigma_3)$. The spectra of $H_a(\mathbf{k})$ and $h_a(\mathbf{k})$ are compared in Fig. 3(a).

We obtain two Dirac points of $H_a(\mathbf{k})$ from $\mathbf{r}(\mathbf{k}) = \mathbf{0}$ which locate at $(0, \pi)$ and $(\pi, 0)$. In the presence of squeezing, the mass term $-(s\text{Re}\xi/\lambda)\sigma_3$ derived from Eq. (28) may open an excitation gap and extremely changes the Berry curvature close to each Dirac cone. The gapped condition of the effective Hamiltonian $h_a(\mathbf{k})$ can be calculated as $|s\text{Re}\xi/\lambda J| \neq 2$. The Chern number of the lower excitation band is given by

$$C = \begin{cases} -\text{sgn}(s\text{Re}\xi/\lambda J), & |s\text{Re}\xi/\lambda J| < 2, \\ 0, & |s\text{Re}\xi/\lambda J| > 2. \end{cases} \quad (30)$$

It equals to the winding number (Brouwer degree [63]) of $\mathbf{r}(\mathbf{k}) - \frac{\text{Re}\xi}{\lambda} \mathbf{s}$ which maps T^2 to $\mathbb{R}^3 \setminus \mathbf{0} \approx S^2$. This model shows that the simplest Dirac-like construction is able to generate nontrivial bosonic BE.

B. \mathbb{Z}_2 -type topological Bogoliubov excitations

Next, we construct a three-dimensional model with time-reversal symmetry, whose topology is characterized by a \mathbb{Z}_2 invariant. Like the above construction, the Hamiltonian in form of Eqs. (26–27) is chosen as [47]

$$\mathbf{r}(\mathbf{k}) = J \left(\sin k_x, \sin k_y, \sin k_z, \sum_{n=x,y,z} \cos k_n + 1 \right), \quad (31)$$

and $\mathbf{s} = (0, 0, 0, s)$. The parameter ξ is set as a real number. The Clifford generators $\boldsymbol{\gamma} = (\gamma_1, \gamma_2, \gamma_3, \gamma_4)$ are

$$\gamma_4 = \begin{pmatrix} I_2 & \\ & -I_2 \end{pmatrix}, \quad \gamma_n = \begin{pmatrix} & \sigma_n \\ \sigma_n & \end{pmatrix}, \quad (32)$$

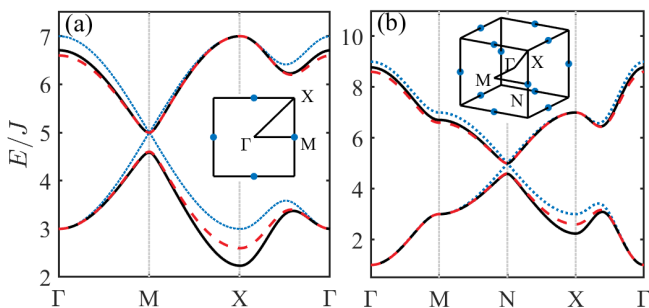


Figure 3. (color online) Band structures of (a) \mathbb{Z} -type and (b) \mathbb{Z}_2 -type topological bosonic BE. The blue dotted lines denote the spectra of $H_a(\mathbf{k})$, while the black solid and red dashed lines denote the exact and approximate spectra of $h_a(\mathbf{k})$, respectively. The approximate result is from Eq. (28). The square and cube denote the Brillouin zones in which the blue dots denote the locations of Dirac points. Parameters are $\lambda = 5J$ and $\xi = s = J$.

where $n = 1, 2, 3$. The Hamiltonian $H(\mathbf{k})$ not only satisfies the particle-hole symmetry Eq. (3) but also respects T symmetry $U_T^{-1}H^*(-\mathbf{k})U_T = H(\mathbf{k})$ with $U_T = I_4 \otimes \sigma_2$. We also confirm that the effective Hamiltonian $h_a(\mathbf{k})$ given by Eq. (28) preserves the T symmetry, i.e., $u_T^{-1}h_a^*(-\mathbf{k})u_T = h_a(\mathbf{k})$ with $u_T = I_2 \otimes \sigma_2$.

Figure 3(b) illustrates the spectra of $H_a(\mathbf{k})$ and $h_a(\mathbf{k})$. There are three Dirac points located at $(0, \pi, \pi)$, $(\pi, 0, \pi)$ and $(\pi, \pi, 0)$. The squeezing-induced mass term opens a gap close to these Dirac cones if $|\xi s/\lambda J - 1| \neq 1, 3$. The effective Hamiltonian $h_a(\mathbf{k})$ thus describes a T -invariant topological insulator. Its energy bands have Kramer's degeneracy so that the Chern number of the lowest bands always vanishes. The corresponding topological feature is characterized by a \mathbb{Z}_2 invariant which is given by

$$\nu = \begin{cases} 1, & |\xi s/\lambda J - 1| \in (1, 3), \\ 0, & |\xi s/\lambda J - 1| \in [0, 1) \cup (3, +\infty). \end{cases} \quad (33)$$

This model shows that the minimal construction is able to generate various types of topological bosonic BEs.

Our construction is potentially realizable in bosonic systems. The platforms like optical lattices with cold atoms [10, 64, 65], magnonic crystals [66–71] and photonic crystals [51, 52, 59, 72, 73] are accessible for the single-particle models. Whereas, the actual challenge for experiments is the realization of the required squeezing interaction. Apart from magnonic materials in which topological gap and Weyl points have been observed with the aid of theoretical calculations [15, 19, 74–76], here we predict that the photonic crystals might be another candidate. The photonic array is made of optically nonlinear materials with second-order nonlinear susceptibility $\chi^{(2)}$. When the system is coherently pumped with the frequency matching condition (i.e., one photon resonantly converting to two photons), the auxiliary mode can be treated classically and the squeezing interaction then emerges [43]. Such a squeezing can be tuned by ad-

justing the amplitude and phase of the pump. And the construction based on \mathbf{k} -independent squeezing interaction would make the implementation easier.

V. CONCLUSIONS

In summary, we have established a framework for the topological analysis and construction of bosonic BdG models in the weak interaction limit. An effective non-interacting Hamiltonian has been derived from a squeezing transformation. After a perturbation truncation, the squeezing interaction has been found to play an essential role as an effective SOC. For the squeezing-induced topological gap opening upon a gapless band dispersion, the effective SOC has further been simplified as a momentum-independent Zeeman coupling. Then the formulation has been applied to two existed models, which gives deeper understandings on their topological structures. Finally, the minimal construction of various types of topological bosonic BEs has also been built based on the Clifford algebra and two concrete examples have been provided, which are applicable for experiments.

Our work opens up the studies of squeezed topological phases in future. Firstly, the squeezing properties of the bulk and edge BE modes could be further investigated based on the squeezing transformation. Since the BdG system can be transformed to a non-interacting one, the bulk-edge correspondence for bosonic system may be strictly established. Secondly, the \mathbb{Z}_2 -type topological bosonic BE has very few examples at the present stage. It is probable to find more examples in photonic crystal and cold atom system with the help of our perturbation formula. Lastly, the topological analysis toward the gapless points in bosonic BE bands is also an interesting topic.

ACKNOWLEDGMENTS

We thank Guang-Quan Luo for helpful discussions and providing detail parameters on the ultracold atom models. This work is supported by National Key R&D Program of China (Grant No. 2018YFA0307200), the Key-Area Research and Development Program of Guangdong Province (Grant No. 2019B030330001), National Natural Science Foundation of China (Grant No. U1801661), and high-level special funds from Southern University of Science and Technology (Grant No. G02206401).

Appendix A: Generic quadratic bosonic model

Here we discuss the generic case that matrix $H(\mathbf{k}) = \begin{pmatrix} H_a & H_s \\ H_s^\dagger & H_b \end{pmatrix}$ has no symmetric constraint. Now the field operator turns to $\hat{\phi}_{\mathbf{k}}^\dagger = (\hat{a}_{\mathbf{k}}^\dagger, \hat{b}_{-\mathbf{k}})$ which contains in-

dependent creation part $\hat{a}_{\mathbf{k}}^\dagger$ and annihilation part $\hat{\mathbf{b}}_{\mathbf{k}} = (\hat{b}_{\mathbf{k},1}, \dots, \hat{b}_{\mathbf{k},N'})$. And the Hamiltonian is written as

$$\hat{H} = \sum_{\mathbf{k}} \hat{\phi}_{\mathbf{k}}^\dagger H(\mathbf{k}) \hat{\phi}_{\mathbf{k}} \quad (\text{A1})$$

without factor 1/2. Physically, this system consists of a pair of bosonic tight-binding models $\sum_{\mathbf{k}} \hat{a}_{\mathbf{k}}^\dagger H_a(\mathbf{k}) \hat{a}_{\mathbf{k}}$ and $\sum_{\mathbf{k}} \hat{\mathbf{b}}_{-\mathbf{k}} H_b(\mathbf{k}) \hat{\mathbf{b}}_{-\mathbf{k}}^\dagger$ coupled by two-mode squeezing interactions $\sum_{\mathbf{k}} \hat{a}_{\mathbf{k}}^\dagger H_s(\mathbf{k}) \hat{\mathbf{b}}_{-\mathbf{k}}^\dagger + \text{h.c.}$. This construction in zero dimension has been widely studied in quantum optics.

Similar to the above treatment, we adopt a new squeeze operator

$$\hat{S} = \exp \sum_{\mathbf{k}} \left[\hat{a}_{\mathbf{k}}^\dagger w(\mathbf{k}) \hat{\mathbf{b}}_{-\mathbf{k}}^\dagger - \text{h.c.} \right] \quad (\text{A2})$$

to achieve the previous transformation

$$\hat{S}^\dagger \hat{H} \hat{S} = \sum_{\mathbf{k}} \hat{\phi}_{\mathbf{k}}^\dagger h(\mathbf{k}) \hat{\phi}_{\mathbf{k}}, \quad h = e^W H e^W, \quad (\text{A3})$$

and keep choosing W by Eq. (10), arriving at block-diagonal matrix $h(\mathbf{k}) = \begin{pmatrix} h_a(\mathbf{k}) & \\ & h_b(\mathbf{k}) \end{pmatrix}$. Eventually, the Hamiltonian in the squeezed state representation consists of two isolated non-interacting systems, given by

$$\hat{S}^\dagger \hat{H} \hat{S} = \sum_{\mathbf{k}} \hat{a}_{\mathbf{k}}^\dagger h_a(\mathbf{k}) \hat{a}_{\mathbf{k}} + \sum_{\mathbf{k}} \hat{\mathbf{b}}_{-\mathbf{k}} h_b(\mathbf{k}) \hat{\mathbf{b}}_{-\mathbf{k}}^\dagger. \quad (\text{A4})$$

The topological information of quadratic bosonic system \hat{H} is fully contained in the effective Hamiltonian $h(\mathbf{k}) = h_a(\mathbf{k}) \oplus h_b(\mathbf{k})$, characterized by two AZ classes. The approximate formula of $h_a(\mathbf{k})$ is still given by Eq. (18) if the system has the squeezing-induced gap. And $h_b(\mathbf{k})$ can be approximated by the same procedure, i.e.,

$$h_b(\mathbf{k}) = H_b(\mathbf{k}) - \left[H_s^\dagger (H_a + \lambda' I)^{-1} H_s \right]_{\mathbf{k}=\mathbf{p}'}, \quad (\text{A5})$$

where (\mathbf{p}', λ') is a band-crossing point of $H_b(\mathbf{k})$.

-
- [1] M. Z. Hasan and C. L. Kane, *Rev. Mod. Phys.* **82**, 3045 (2010).
- [2] X.-L. Qi and S.-C. Zhang, *Rev. Mod. Phys.* **83**, 1057 (2011).
- [3] C.-K. Chiu, J. C. Y. Teo, A. P. Schnyder, and S. Ryu, *Rev. Mod. Phys.* **88**, 035005 (2016).
- [4] B. A. Bernevig, *Topological Insulators and Topological Superconductors* (Princeton University Press, 2013).
- [5] M. Sato and Y. Ando, *Rep. Prog. Phys.* **80**, 076501 (2017).
- [6] T. Karzig, C.-E. Bardyn, N. H. Lindner, and G. Refael, *Phys. Rev. X* **5**, 031001 (2015).
- [7] Z. Yang, F. Gao, X. Shi, X. Lin, Z. Gao, Y. Chong, and B. Zhang, *Phys. Rev. Lett.* **114**, 114301 (2015).
- [8] D. Jin, L. Lu, Z. Wang, C. Fang, J. D. Joannopoulos, M. Soljačić, L. Fu, and N. X. Fang, *Nat. Commun.* **7**, 13486 (2016).
- [9] T. Ozawa, H. M. Price, A. Amo, N. Goldman, M. Hafezi, L. Lu, M. C. Rechtsman, D. Schuster, J. Simon, O. Zilberberg, and I. Carusotto, *Rev. Mod. Phys.* **91**, 015006 (2019).
- [10] D.-W. Zhang, Y.-Q. Zhu, Y. X. Zhao, H. Yan, and S.-L. Zhu, *Adv. Phys.* **67**, 253 (2018).
- [11] L. Zhang, J. Ren, J.-S. Wang, and B. Li, *Phys. Rev. B* **87**, 144101 (2013).
- [12] R. Shindou, J.-i. Ohe, R. Matsumoto, S. Murakami, and E. Saitoh, *Phys. Rev. B* **87**, 174402 (2013).
- [13] R. Shindou, R. Matsumoto, S. Murakami, and J.-i. Ohe, *Phys. Rev. B* **87**, 174427 (2013).
- [14] R. Shindou and J.-i. Ohe, *Phys. Rev. B* **89**, 054412 (2014).
- [15] R. Chisnell, J. S. Helton, D. E. Freedman, D. K. Singh, R. I. Bewley, D. G. Nocera, and Y. S. Lee, *Phys. Rev. Lett.* **115**, 147201 (2015).
- [16] K. Li, C. Li, J. Hu, Y. Li, and C. Fang, *Phys. Rev. Lett.* **119**, 247202 (2017).
- [17] X. S. Wang, Y. Su, and X. R. Wang, *Phys. Rev. B* **95**, 014435 (2017).
- [18] K. Nakata, S. K. Kim, J. Klinovaja, and D. Loss, *Phys. Rev. B* **96**, 224414 (2017).
- [19] P. A. McClarty, F. Krüger, T. Guidi, S. F. Parker, K. Refson, A. W. Parker, D. Prabhakaran, and R. Coldea, *Nat. Phys.* **13**, 736 (2017).
- [20] P. A. McClarty, X.-Y. Dong, M. Gohlke, J. G. Rau, F. Pollmann, R. Moessner, and K. Penc, *Phys. Rev. B* **98**, 060404 (2018).
- [21] F. Lu and Y.-M. Lu, "Magnon band topology in spin-orbital coupled magnets: classification and application to α -rucl₃," (2018), [arXiv:1807.05232 \[cond-mat.str-el\]](https://arxiv.org/abs/1807.05232).
- [22] H. Kondo, Y. Akagi, and H. Katsura, *Phys. Rev. B* **99**, 041110 (2019).
- [23] H. Kondo, Y. Akagi, and H. Katsura, *Phys. Rev. B* **100**, 144401 (2019).
- [24] S. A. Díaz, J. Klinovaja, and D. Loss, *Phys. Rev. Lett.* **122**, 187203 (2019).
- [25] C.-E. Bardyn, T. Karzig, G. Refael, and T. C. H. Liew, *Phys. Rev. B* **93**, 020502 (2016).
- [26] V. Peano, M. Houde, C. Brendel, F. Marquardt, and A. A. Clerk, *Nat. Commun.* **7**, 10779 (2016).
- [27] G. Engelhardt, M. Benito, G. Platero, and T. Brandes, *Phys. Rev. Lett.* **117**, 045302 (2016).
- [28] G. Engelhardt and T. Brandes, *Phys. Rev. A* **91**, 053621 (2015).
- [29] S. Furukawa and M. Ueda, *New J. Phys.* **17**, 115014 (2015).
- [30] Z.-F. Xu, L. You, A. Hemmerich, and W. V. Liu,

- Phys. Rev. Lett.* **117**, 085301 (2016).
- [31] M. Di Liberto, A. Hemmerich, and C. Morais Smith, *Phys. Rev. Lett.* **117**, 163001 (2016).
- [32] G.-Q. Luo, A. Hemmerich, and Z.-F. Xu, *Phys. Rev. A* **98**, 053617 (2018).
- [33] P. Ring and P. Schuck, *The Nuclear Many-Body Problem* (Springer, New York, 1980).
- [34] J. P. Blaizot and G. Ripka, *Quantum Theory of Finite Systems* (MIT Press, Cambridge, MA, 1986).
- [35] J. H. P. Colpa, *Physica A* **134**, 417 (1986).
- [36] A. Altland and M. R. Zirnbauer, *Phys. Rev. B* **55**, 1142 (1997).
- [37] A. Kitaev, *AIP Conf. Proc.* **1134**, 22 (2009).
- [38] M. Stone, C.-K. Chiu, and A. Roy, *J. Phys. A: Math. Theor.* **44**, 045001 (2011).
- [39] G. De Nittis and K. Gomi, *Rev. Math. Phys.* **31**, 1950003 (2019).
- [40] M. Lein and K. Sato, *Phys. Rev. B* **100**, 075414 (2019).
- [41] Z. Zhou, L.-L. Wan, and Z.-F. Xu, “Classification of topological excitations in quadratic bosonic systems,” (2019), [arXiv:1905.07989 \[cond-mat.quant-gas\]](https://arxiv.org/abs/1905.07989).
- [42] M. Malki and G. S. Uhrig, *Phys. Rev. B* **99**, 174412 (2019).
- [43] M. O. Scully and M. S. Zubairy, *Quantum Optics* (Cambridge University Press, 1997).
- [44] R. Simon, S. Chaturvedi, and V. Srinivasan, *J. Math. Phys.* **40**, 3632 (1999).
- [45] C. L. Kane and E. J. Mele, *Phys. Rev. Lett.* **95**, 146802 (2005).
- [46] C. L. Kane and E. J. Mele, *Phys. Rev. Lett.* **95**, 226801 (2005).
- [47] B. A. Bernevig and S.-C. Zhang, *Phys. Rev. Lett.* **96**, 106802 (2006).
- [48] L. Fu, C. L. Kane, and E. J. Mele, *Phys. Rev. Lett.* **98**, 106803 (2007).
- [49] M. Atiyah, R. Bott, and A. Shapiro, *Topology* **3**, 3 (1964).
- [50] R. Rossignoli and A. M. Kowalski, *Phys. Rev. A* **72**, 032101 (2005).
- [51] M. Notomi, E. Kuramochi, and T. Tanabe, *Nat. Photonics* **2**, 741 (2008).
- [52] B. J. Eggleton, B. Luther-Davies, and K. Richardson, *Nat. Photonics* **5**, 141 (2011).
- [53] M. Aidelsburger, M. Atala, M. Lohse, J. T. Barreiro, B. Paredes, and I. Bloch, *Phys. Rev. Lett.* **111**, 185301 (2013).
- [54] M. Aidelsburger, M. Lohse, C. Schweizer, M. Atala, J. Barreiro, S. Nascimbène, N. Cooper, I. Bloch, and N. Goldman, *Nat. Phys.* **11**, 162 (2014).
- [55] Y. Yan and Q. Zhou, *Phys. Rev. Lett.* **120**, 235302 (2018).
- [56] S. Lieu, *Phys. Rev. B* **98**, 115135 (2018).
- [57] B. A. Bernevig, T. L. Hughes, and S.-C. Zhang, *Science* **314**, 1757 (2006).
- [58] L. Fu and C. L. Kane, *Phys. Rev. B* **76**, 045302 (2007).
- [59] J. D. Joannopoulos, S. G. Johnson, J. N. Winn, and R. D. Meade, *Photonics Crystals: Modeling the flow of light* (Princeton University Press, 2011).
- [60] K. Ohgushi, S. Murakami, and N. Nagaosa, *Phys. Rev. B* **62**, R6065 (2000).
- [61] G. E. Volovik, *The Universe in a Helium Droplet* (Oxford University Press, 2003).
- [62] X.-L. Qi, Y.-S. Wu, and S.-C. Zhang, *Phys. Rev. B* **74**, 045125 (2006).
- [63] L. E. J. Brouwer, *Mathematische Annalen* **71**, 598 (1912).
- [64] D. Jaksch, C. Bruder, J. I. Cirac, C. W. Gardiner, and P. Zoller, *Phys. Rev. Lett.* **81**, 3108 (1998).
- [65] V. I. Yukalov, *Laser Phys.* **19**, 1 (2009).
- [66] R. Matsumoto and S. Murakami, *Phys. Rev. Lett.* **106**, 197202 (2011).
- [67] Y. V. Gulyaev, S. A. Nikitov, L. V. Zhivotovskii, A. A. Klimov, P. Tailhades, L. Presmanes, C. Bonningue, C. S. Tsai, S. L. Vysotskii, and Y. A. Filimonov, *Journal of Experimental and Theoretical Physics Letters* **77**, 567 (2002).
- [68] N. Singh, S. Goolaup, and A. O. Adeyeye, *Nanotechnology* **15**, 1539 (2004).
- [69] C. C. Wang, A. O. Adeyeye, and N. Singh, *Nanotechnology* **17**, 1629 (2006).
- [70] B. Lenk, H. Ulrichs, F. Garbs, and M. Münzenberg, *Phys. Rep.* **507**, 107 (2011).
- [71] A. O. Adeyeye and N. Singh, *J. Phys. D: Appl. Phys.* **41**, 153001 (2008).
- [72] Z. Wang, Y. Chong, J. D. Joannopoulos, and M. Soljačić, *Nature* **461**, 772 (2009).
- [73] C. Wang and T. Senthil, *Phys. Rev. B* **87**, 235122 (2013).
- [74] S. Bao, J. Wang, W. Wang, Z. Cai, S. Li, Z. Ma, D. Wang, K. Ran, Z.-Y. Dong, D. L. Abernathy, S.-L. Yu, X. Wan, J.-X. Li, and J. Wen, *Nat. Commun.* **9**, 2591 (2018).
- [75] W. Yao, C. Li, L. Wang, S. Xue, Y. Dan, K. Iida, K. Kamazawa, K. Li, C. Fang, and Y. Li, *Nature Physics* **14**, 1011 (2018).
- [76] L. Chen, J.-H. Chung, B. Gao, T. Chen, M. B. Stone, A. I. Kolesnikov, Q. Huang, and P. Dai, *Phys. Rev. X* **8**, 041028 (2018).